Tenascin-C secreted by transdifferentiated retinal pigment epithelial cells promotes choroidal neovascularization via integrin αV

小林, 義行

https://doi.org/10.15017/1806917

出版情報：九州大学, 2016, 博士（医学）, 課程博士
バージョン：
権利関係：やむを得ない事由により本文ファイル非公開（2）

Tenascin-C secreted by transdifferentiated retinal pigment epithelial cells promotes choroidal neovascularization via integrin α_V

Yoshiyuki Kobayashi[1], Shigeo Yoshida[1], Yedi Zhou[1], Takahito Nakama[1], Keijiro Ishikawa[1], Yuki Kubo[1], Mitsuru Arima[1], Shintaro Nakao[1], Toshio Hisatomi[1], Yasuhiro Ikeda[1], Akira Matsuda[2], Koh-Hei Sonoda[1], and Tatsuro Ishibashi[1]

[1]Department of Ophthalmology, Kyushu University Graduate School of Medical Sciences, Fukuoka 812-8582, Japan

[2]Department of Ophthalmology, Juntendo University, Tokyo 113-8431, Japan

Short running title: RPE-derived tenascin-C promotes CNV

Sources of support: This study was supported by Grants-in-Aid for Scientific Research (B) (No. 15H04995 and 26293374), a Grant-in-Aid for Challenging Exploratory Research (No. 26670757), and a Grant-in-Aid for JSPS Fellows from Japan Society for the Promotion of Science (No.15J03433).

Correspondence: Shigeo Yoshida, MD, PhD

Department of Ophthalmology, Kyushu University Graduate School of Medical Sciences, Fukuoka 812-8582, Japan.

Telephone: 81-92-642-5648

Fax: 81-92-642-5663

E-mail: yosida@eye.med.kyushu-u.ac.jp

Abstract

Tenascin-C is expressed in choroidal neovascular (CNV) membranes in eyes with age-related macular degeneration (AMD). However, its role in the pathogenesis of CNV remains to be elucidated. Here, we investigated the role of tenascin-C in CNV formation. In immunofluorescence analyses, tenascin-C co-stained with α-SMA, pan-cytokeratin, CD31, CD34, and integrin α_V in the CNV membranes of patients with AMD and a mouse model of laser-induced CNV. A marked increase in the expression of tenascin-C mRNA and protein was observed 3 days after laser photocoagulation in the mouse CNV model. Tenascin-C was also shown to promote proliferation and inhibit adhesion of human retinal pigment epithelial (hRPE) cells *in vitro*. Moreover, tenascin-C promoted proliferation, adhesion, migration, and tube formation in human microvascular endothelial cells (HMVECs); these functions were, however, blocked by cilengitide, an integrin α_V inhibitor. Exposure to TGF-β2 increased tenascin-C expression in hRPE cells. Conditioned media harvested from TGF-β2-treated hRPE cell cultures enhanced HMVEC proliferation and tube formation, which were inhibited by pretreatment with tenascin-C siRNA. The CNV volume was significantly reduced in tenascin-C knock-out mice and tenascin-C siRNA-injected mice. These findings suggest that tenascin-C is secreted by transdifferentiated RPE cells and promotes the development of CNV via integrin α_V in a paracrine manner. Therefore, tenascin-C could be a potential therapeutic target for the inhibition of CNV development associated with AMD.

Key words: tenascin-C, angiogenesis, age-related macular degeneration

Age-related macular degeneration (AMD) is one of the leading causes of vision reduction in older people in developed countries.[1] The decrease in visual acuity is usually attributed to choroidal neovascularization (CNV), a pathological invasion of new blood vessels into the subretinal space from the choriocapillaris through the Bruch's membrane. The development of these vessels is accompanied by retinal edema, retinal detachment, and hemorrhage, which destroys photoreceptor cells.[2]

Recently, a number of studies have focused on the effects of anti-vascular endothelial growth factor (VEGF) treatment on CNV in eyes with AMD.[3-6] Monthly intravitreal injections of ranibizumab, an anti-VEGF agent, prevented vision reduction in nearly 95% of the AMD patients, and significantly improved the vision in 40% of the patients, for 2 years.[3] However, the use of anti-VEGF drugs to maintain vision over long periods of time causes problems in tolerance or tachyphylaxis, which is a reduction in drug efficacy following repeated administration.[7-9] Approximately 18.3% of all AMD patients treated with anti-VEGF drugs reportedly develop geographic atrophy within 2 years of beginning the treatment.[10] Therefore, many research efforts are now directed towards the identification of new agents that could be effective in the treatment of CNV.

We and others have reported that tenascin-C promotes the retinal neovascularization associated with proliferative diabetic retinopathy.[11-13] Tenascin-C is a large hexameric extracellular glycoprotein composed of 180–320 kDa monomers. It consists of four major domains: a globular N-terminal assembly domain, a 14.5 epidermal growth factor-like repeats domain, a fibronectin type III–like repeat domain, and a fibrinogen-like

sequence. Fibronectin type III–like repeats of tenascin-C affect cell adhesion via integrin receptors and Annexin II.[14] Tenascin-C is chiefly expressed during development, but is also present at low levels in most adult tissues. However, tenascin-C is continuously up-regulated during active inflammation and tissue repair.[15] Several studies have reported that tenascin-C plays a vital role in cardiac ischemia,[16-18] tumor angiogenesis, and metastasis.[19-22] Moreover, it has been reported that CNV membranes obtained from patients with AMD containing retinal pigment epithelial (RPE) cells express tenascin-C.[23, 24]

We have recently reported that periostin, a matricellular protein produced by RPE cells, promotes CNV formation.[25] However, the angiogenic processes mediated by tenascin-C in the pathogenesis of CNV have not been elucidated.

Therefore, the purpose of this study was to investigate the expression and function of tenascin-C in human CNV membranes in an *in vivo* mouse CNV model as well as RPE and vascular endothelial cells *in vitro*. We also evaluated the efficacy of tenascin-C as a potential therapeutic target using acute tenascin-C blockade in a mouse CNV model.

Materials and Methods

Human specimens

This study was approved by the Ethics Committee of Kyushu University Hospital; the surgical specimens were handled in accordance with the Declaration of Helsinki. Signed

informed consent forms were obtained from all patients prior to the surgical procedure. CNV membranes were surgically removed from 3 eyes of 3 patients with wet-type AMD. The ages of these patients at the time of pars plana vitrectomy ranged from 62 to 81 years.

Animals

All animal experiments were approved by the Ethics Committee for Animal Experiments of the Kyushu University Graduate School of Medical Sciences. C57BL/6J mice were purchased from CLEA Japan, Inc. (Tokyo, Japan) and tenascin-C knock-out mice were purchased from the RIKEN BioResource Center (Ibaraki, Japan). Tenascin-C knock-out mice are also known as rd8/rd8 mice as they carry the *Crb1* gene, which is associated with retinal degeneration;[26] therefore, the rd8/rd8 mutation was bred out by backcrossing the knock-out mice with the C57BL/6J line.

Mouse model of CNV

The Bruch's membrane was ruptured by laser photocoagulation to generate CNV in mice.[27] Briefly, 7 week-old male C57BL/6J and tenascin-C knock-out mice were anesthetized, and their pupils were dilated with 0.5% tropicamide. Four burns were produced on each retina by a 532-nm diode laser (75 μm spot size, 0.1 second duration, 100 mW) of a slit-lamp-delivery system in a photocoagulator (Novus Verdi; Coherent Inc., Santa Clara, CA).

The effect of tenascin-C siRNA was evaluated *in vivo* by injecting tenascin-C or control siRNA (#4390843: Thermo Fisher Scientific, Waltham, MA) with randomly scrambled sequences into the eye immediately after laser photocoagulation.

Immunofluorescence staining

Immunohistochemistry was performed as described previously.[28, 29] Briefly, as the number of AMD patients for surgery was limited, CNV membranes from clinical samples were embedded in paraffin and cut into 3-μm sections for long-term sample preservation. The sections were deparaffinized, rehydrated, blocked, and finally incubated overnight with primary antibodies. The sections were subsequently incubated with secondary antibodies for 30 minutes at room temperature. For immunofluorescence analysis in mice, the eyeballs of mice with photocoagulation (5 days after laser-treatment) were embedded in OCT compound (Tissue-Tek; Sakura Seiki, Tokyo, Japan) and frozen on dry ice. The frozen mouse eyes were cryosectioned to a thickness of 10-μm, fixed in -20°C acetone for 10 minutes, blocked with 5% skim milk, and subsequently incubated overnight with the primary antibody. Finally, the sections were incubated with the secondary antibody for 20 minutes at room temperature. The antibodies are listed in the Supplementary Table 1 and 2. The nuclei were counterstained with Hoechst 33342 (H3570: 1:400 dilution; Life Technologies, Gaithersburg, MD), and the sections were examined with a fluorescence microscope (BZ-9000; Keyence, Osaka, Japan).

Quantification of CNV volume in mouse model

The eyes were removed 7 days after photocoagulation and fixed in 4% paraformaldehyde for 1 hour. The cornea, lens, and retina were removed, and the choroid/sclera segment was fixed for 24 hours in 4% paraformaldehyde. The tissue was exposed to methanol for 20 minutes, treated with 0.1% Triton X-100 (Sigma-Aldrich, St. Louis, MO) in PBS for 1 hour, incubated in fluorescein-labeled isolectin B4 (FL1201; 1:200 dilution; Vector Laboratories, Burlingame, CA) at room temperature for 1.5 hours, and then flat-mounted on glass slides. Choroidal flat mounts were observed with a laser scanning confocal microscope (Nikon A1R; Nikon, Tokyo, Japan), and the volume at each burn site was measured using the NIS-Elements software (Nikon).

Cell culture

Human retinal pigment epithelial cells (hRPE, 00194987; Lonza Walkersville, Walkersville, MD) were cultured in Dulbecco's modified Eagle's medium (DMEM) with 100 U/mL penicillin, 100 µg/mL streptomycin, and 10% heat-inactivated fetal bovine serum (FBS). Human dermal microvascular endothelial cells (HMVECs, CC-2543; Lonza Walkersville) were cultured in EGM-2MV BulletKit (CC-3202; Lonza Walkersville).

The hRPE cells were seeded in collagen-coated 24-well plates for mRNA assays and 6-well plates for protein assays. The cells were starved in serum-free DMEM for 24 hours, and subsequently treated with or without TGF-β2 (SRP3170; Sigma-Aldrich) for 24 hours. mRNA was then extracted from these cells using TRIzol reagent (Life

Technologies). The supernatant (containing the proteins) was collected after a 48-h incubation period, and total cell lysate was extracted with a lysis buffer.

Cilengitide (10 μM; Selleckchem, Huston, TX) was added at the time of stimulation in all subsequent assays to inhibit integrin $\alpha_V\beta_3$ and $\alpha_V\beta_5$.

Real-time qRT-PCR

The tenascin-C (and GAPDH control) mRNA expression was quantified by qRT-PCR, as described previously.[25, 30] Briefly, total RNA was extracted and reverse-transcribed with a first-strand cDNA synthesis kit (Roche, Mannheim, Germany). The level of gene expression was determined by real-time RT-PCR using a Roche LightCycler 96 (Roche). The quantification was carried out using either a TaqMan-probe or SYBR Green. The primers and annealing temperatures used are listed in Supplemental Table 3.

Enzyme-linked Immunosorbent Assay (ELISA)

The protein concentration of tenascin-C was measured by sandwich ELISA using a standard ELISA kit (27767; IBL, Gunma, Japan) in compliance with the manufacturer protocol. The samples were added to a buffer solution in 96-well plates and incubated for 1 hour at room temperature. The solution was aspirated and washed. The wells were then incubated with horseradish peroxidase-conjugated mouse monoclonal antibody against tenascin-C (4F10TT) for 30 minutes at 4°C. The solution was aspirated and washed again. The substrate solution was added to each well and the plate was

incubated for 30 minutes at room temperature. The stop solution was added to each well and the plate was read with a microplate reader (ImmunoMini NJ-2300; NJ InterMed, Tokyo, Japan) at 450 nm.

Western blot analysis

The protein samples were separated on a NuPAGE 3-8% Tris-Acetate gel (EA0375; Life Technologies) and the blots were incubated with a monoclonal antibody against tenascin-C (4F10TT: 10337: 1:3000; IBL). The blot was developed by an immunoperoxidase method (Envision+; Dako, Glostrup, Denmark) and subsequently visualized using a SuperSignal West Femto maximum sensitivity substrate (#34095; Thermo Fisher Scientific). Lane-loading differences were normalized by blotting the membranes with an antibody against β-actin (#4970: 1:5000; Cell Signaling Technologies, Beverly, MA).

Cell proliferation assay

Proliferation of the hRPE cells and HMVECs was analyzed by bromodeoxyuridine (BrdU)-incorporated ELISA (Roche) according to the manufacturer protocol, with a 1.5-h BrdU incubation.

Cell adhesion assay

The cell adhesion assay was performed as described in a previous report.[31] Briefly, hRPE cells were trypsinized and resuspended in serum-free DMEM containing recombinant tenascin-C. Cell suspension (1×10^4 cells/200 μL) was added to each

fibronectin-coated well (F2006: 10 μg/mL; Sigma-Aldrich) and allowed to attach for 1 hour. HMVECs (1×10^4 cells/200 μL) were resuspended in EBM-2 media with 0.5% FBS containing recombinant tenascin-C, and allowed to attach for 12 hours. The cells were gently washed twice with PBS, fixed with 4% PFA, and stained with Hoechst 33342 (H3570, 1:1000 dilution; Life Technologies) for 15 minutes. The stained cells were counted with a 4× objective lens in four fields, and the data was analyzed with the ImageJ software (National Institute of Health, Bethesda, MD).

Cell migration assay

The effect of tenascin-C on the migration of HMVECs was examined by performing transwell assays using cell culture inserts with a pore size of 8-μm (Corning, Corning, NY). HMVECs were suspended at a concentration of 5×10^4 cells/mL in EBM-2 media supplemented with 0.5% FBS and recombinant tenascin-C. To assess cell migration, HMVECs stimulated with tenascin-C were placed in the upper chamber and allowed to migrate to the reverse side of the membrane. The inserts were fixed with 4% PFA and stained with Hoechst 33342 (H3570, 1:1000 dilution; Life Technologies) for 15 minutes. The stained cells were counted in four random fields under a 20× objective lens, and the data was analyzed using ImageJ software (National Institute of Health).

Tube formation assay

HMVECs were plated at a concentration of 1×10^4 cells/well in 96-well plates pre-coated with Matrigel Basement Membrane Matrix (BD Bioscience), in EBM-2 media containing 0.5% FBS and recombinant tenascin-C. The cells were subsequently

incubated for 12 hours at 37°C. The data was analyzed using ImageJ software (National Institute of Health).

Preparation of hRPE-conditioned medium

hRPE-conditioned medium was produced by culturing hRPE cells in 6-well plates to a confluence of 70–80%. Tenascin-C siRNA (10 nM) or control siRNA (10 nM) was mixed with 4 μL Lipofectamine RNAiMAX (Thermo Fisher Scientific) in 2 mL Opti-MEM (Thermo Fisher Scientific). This mixture was added to hRPE cells and the cells were incubated for 24 hours. Recombinant TGF-β2 was added at a concentration of 10 ng/mL per well and incubated for 24 hours. The composite transfection medium was removed and replaced with serum-free EBM-2. After 24 hours, conditioned medium was collected from the 6-well plates and filtered through 40-μm filters (Corning).

Statistical analyses

All results are expressed as the means ± standard errors of means (SEMs). The differences among groups were analyzed by two-tailed Student's *t* tests or one-way analysis of variance (ANOVA) with Dunnett's tests or Tukey tests. Statistical analyses were performed with a commercial statistical software package (JMP v.11.0; SAS Institute, Cary, NC). A *P*-value <0.05 was taken to be statistically significant.

Results

Tenascin-C is expressed by RPE cells transdifferentiated into myofibroblasts in CNV membranes

The location of tenascin-C in CNV membranes obtained from the eyes of AMD patients were determined by staining the sections with antibodies against tenascin-C, α-smooth muscle actin (α-SMA), pan-cytokeratin, and CD34, which are markers for myofibroblasts, RPE cells, and vascular endothelial cells, respectively. In the CNV membranes, RPE cells and myofibroblasts were co-localized with tenascin-C. Alternately, vascular endothelial cells were localized around tenascin-C (Figure 1a).

Tenascin-C is expressed by RPE cells transdifferentiated into myofibroblasts in a laser CNV mouse model

The location of tenascin-C in CNV lesions was further determined by immunofluorescent staining for tenascin-C, pan-cytokeratin, α-SMA, CD31, F4/80, and integrin α_V in the mouse CNV model 5 days after the retinal laser photocoagulation. CD31, F4/80, and integrin α_V are markers for vascular endothelial cells, macrophages, and the tenascin-C receptor, respectively. The RPE cells were found to co-localize with tenascin-C as well as α-SMA, whereas vascular endothelial cells partly co-localized with tenascin-C and integrin α_V. In contrast, macrophages co-localized weakly with tenascin-C. These findings indicate that tenascin-C is predominantly expressed in myofibroblasts transdifferentiated from RPE cells, and is bound to vascular endothelial cells via integrin α_V in the CNV lesions (Figure 1b)

Synthesis and secretion of tenascin-C is induced in mouse CNV model

The time course of tenascin-C expression during CNV formation was confirmed by evaluating the mRNA and protein expression of tenascin-C in RPE-choroid tissues obtained from the mouse CNV model at different times. Real-time qRT-PCR showed that the expression of tenascin-C was highly up-regulated in the RPE-choroid at days 1 and 3 after laser coagulation, and decreased thereafter (Figure 2a). The kinetics of protein expression were similar, with peak levels observed at day 3, and markedly reduced protein levels from day 5 (Figure 2b, c). The 4F10TT antibody, which recognizes all tenascin-C variants, identified two isoforms of tenascin-C (210 and 250 kDa). Both the larger and smaller tenascin-C isoforms were expressed in the mouse CNV model.

Synthesis and secretion of tenascin-C is also induced in transdifferentiated hRPE cells stimulated by TGF-β2

Based on the expression of tenascin-C in α-SMA-positive RPE cells, we hypothesized that TGF-β2-induced transdifferentiation of RPE cells into myofibroblasts might lead to tenascin-C production. This theory was tested by evaluating the expression of tenascin-C in hRPE cells exposed to recombinant TGF-β2. We have shown that TGF-β2 caused the cells to become elongated, spindle-shaped, and flat, resembling fibroblasts.[32] Real-time qRT-PCR analysis showed that 1, 3, and 10 ng/mL TGF-β2 induced an up-regulation in the mRNA and protein expression of tenascin-C in hRPE cells in a dose-dependent manner (Figure 2d, e). Consistently, western blot analysis indicated that tenascin-C protein expression was up-regulated in the cell lysates of hRPE cells exposed to TGF-β2 (Figure 2f). The 4F10TT antibody identified two isoforms of

tenascin-C, weighing 210 kDa and 300 kDa. Both of these isoforms were expressed in hRPE cells.

Tenascin-C promotes proliferation and reduces adhesion of hRPE cells

The effect of tenascin-C on hRPE cell function was tested by evaluating the effect of tenascin-C on hRPE cell proliferation and adhesion. Incubation with 30, 100, and 300 μg/mL tenascin-C significantly promoted hRPE cell proliferation, as indicated by increased BrdU incorporation, in a dose-dependent manner (Figure 3a). Recombinant tenascin-C also significantly inhibited the adhesion of hRPE cells to fibronectin-coated wells, which was indicated by the number of stained cells (Figure 3b, c). These results demonstrated that tenascin-C promotes proliferation and reduces adhesion of hRPE cells in an autocrine manner.

Tenascin-C promotes HMVEC proliferation, adhesion, migration, and tube formation

The contribution of tenascin-C to angiogenesis of HMVECs, including cell proliferation, adhesion, migration, and tube formation, was also tested. Exposure to 100 and 300 ng/mL tenascin-C significantly up-regulated the HMVEC proliferation (Figure 3d); additionally, 30, 100, and 300 ng/mL recombinant tenascin-C significantly enhanced the adhesion of HMVECs to fibronectin-coated wells in a dose-dependent manner (Figure 3e, f). In the cell migration assay, 300 ng/mL tenascin-C was shown to significantly promote cell migration (Figure 3g), whereas the same quantity of tenascin-C was shown to significantly promote tube formation in the tube formation assay (Figure 3h, i).

Tenascin-C-dependent angiogenesis is mediated by integrin α_V

To determine whether the tenascin-C-dependent HMVEC proliferation, adhesion, migration, and tube formation are mediated by α_V integrin, we evaluated the inhibitory effect of cilengitide, an integrin $\alpha_V\beta_3$ and integrin $\alpha_V\beta_5$ inhibitor, on HMVECs. Integrin α_V inhibition almost completely suppressed the tenascin-C-induced proliferation, adhesion, migration, and tube formation in HMVECs (Figure 4a–f). These results indicated that integrin α_V mediates the tenascin-C stimulation of proliferation, adhesion, migration, and tube formation in HMVECs.

Tenascin-C secreted from transdifferentiated hRPE cells promotes angiogenesis

We hypothesized that tenascin-C secreted from transdifferentiated hRPE cells induces angiogenesis in a paracrine manner. This hypothesis was tested using a synthesized tenascin-C siRNA (Supplementary Table 4). To confirm the inhibitory effect of tenascin-C siRNA on the expression of tenascin-C in hRPE cells, we examined the production of tenascin-C in hRPE cells cultured with tenascin-C siRNA or control siRNA in the presence or absence of TGF-β2, which is expressed in CNV membranes.[33] Without TGF-β2 stimulation, we observed no significant difference between cells transfected with tenascin-C or control siRNA. In contrast, in the presence of TGF-β2 stimulation, tenascin-C siRNA significantly inhibited the expression of tenascin-C (Figure 5a).

To confirm that tenascin-C secreted from hRPE cells can promote CNV, we assessed the proliferation and tube formation of HMVECs cultured in hRPE-conditioned medium.

hRPE-conditioned medium pretreated with TGF-β2 significantly promoted HMVEC proliferation and tube formation on Matrigel (Figure 5b–d). In contrast, HMVECs cultured in hRPE-conditioned medium pretreated with tenascin-C siRNA and TGF-β2 showed a significant reduction in proliferation and tube formation, compared to those cultured in hRPE pretreated with control siRNA and TGF-β2 (Figure 5b–d). These results indicated that tenascin-C from transdifferentiated hRPE cells facilitates CNV formation.

Disruption of tenascin-C suppresses CNV formation in a mouse CNV model

The involvement of tenascin-C in CNV formation was confirmed by measuring the volume of CNV in the laser-induced tenascin-C knock-out and wild-type C57BL/6J CNV mouse models. The CNV volume, measured in lectin-stained choroidal flat mounts, was significantly reduced to 53% in tenascin-C knock-out mice compared to that seen in wild-type mice at day 7 (Figure 6a–b).

Finally, the possible therapeutic effect of tenascin-C siRNA was assessed by administering C57BL/6J mice with an intravitreous injection of 1, 10, and 100 μM tenascin-C or control siRNA following the laser injury. Ten and hundred μM tenascin-C siRNA induced a significant reduction in CNV volume (63 and 51%) compared to that induced by the control siRNA (Figure 6c, d).

Discussion

Our results showed that the induction of tenascin-C in the laser-induced mouse CNV model reached a peak at day 3 post-laser photocoagulation. Tenascin-C is expressed by RPE cells that have transdifferentiated into myofibroblasts in both the laser-induced mouse CNV model and CNV membranes from AMD patients. Together with the proliferation, migration, and tube formation of HMVECs, tenascin-C may be chronically expressed and may promote CNV membrane formation in AMD patients.

Several studies have reported that myofibroblasts are the major source of tenascin-C in the heart, colon, and liver.[34-36] Consistent with this data, the immunohistochemical experiments performed in this study showed that tenascin-C was co-localized in the myofibroblasts and RPE cells of CNV membranes. Previous immunohistochemical findings in eyes with AMD showed intracellular distribution of TGF-β2 in RPE cells, the predominant isoform in the retina, RPE cells, and CNV membranes.[33, 37] In addition, TGF-β2 is a cytokine of M2 macrophages identified in the CNV membrane. [38, 39] As TGF-β2 contributes to the transdifferentiation of RPE cells into myofibroblasts,[40, 41] TGF-β2 may be a potent inducer of tenascin-C in CNV membranes. Our *in vitro* assays showed that TGF-β2 induced the expression of tenascin-C in hRPE cells, which in turn promoted angiogenesis. These results demonstrate that myofibroblasts transdifferentiated from RPE cells via RPE- and/or M2 macrophage-derived TGF-β2 and continuously produced tenascin-C, resulting in CNV formation in a paracrine manner.

We also found that tenascin-C inhibited the adhesion of hRPE cells and promoted the proliferation of hRPE cells and vascular endothelial cells. Together with the proliferation, migration, and tube formation of HMVECs, these results suggest that tenascin-C promotes tissue remodeling close to the RPE-choroid interface by weakening the RPE cell adhesion to Bruch's membrane, and facilitates the invasion of vessels, to form CNV in the subretinal space. Our findings are consistent with a previously proposed hypothesis that the cell and cytokine activity during CNV formation is very similar to that of wound healing.[42] Active phase CNV contains a number of RPE cells, fibroblasts, and macrophages, which produce proangiogenic cytokines and extracellular matrix proteins, including tenascin-C and periostin.[25, 42]

In the immunohistochemical studies, vascular endothelial cells were co-stained with tenascin-C and integrin α_V. Integrin α_V is expressed in many types of cells. Integrin $\alpha_V\beta_3$ is a well-known receptor that is specifically involved in CNV[43] and is one of the tenascin-C-binding receptors on vascular endothelial cells.[11] Our results demonstrated that cilengitide inhibited cellular proliferation, adhesion, migration, and tube formation in HMVECs treated with tenascin-C. This was consistent with the results of a previous study where tenascin-C was shown to bind to human umbilical vein endothelial cells in the presence of integrin $\alpha_V\beta_3$.[44] Together, these findings suggest that tenascin-C promotes CNV formation by binding to integrin $\alpha_V\beta_3$.

There were some limitations to our study. Although laser-induced mouse models are widely used as models of CNV, it is an acute injury model and therefore may not be an

accurate model of CNV in AMD because the latter CNV occurs as a secondary response to chronic inflammatory processes.[45] The reason why tenascin-C was transiently expressed in the laser-induced model may be that laser-induced CNV is largest by 7 days after photocoagulation and spontaneously diminishes thereafter in this model.[27] In contrast, in AMD patients, our immunofluorescent staining and the findings of previous studies demonstrated that tenascin-C is expressed by transdifferentiated RPE cells (myofibroblasts) at the RPE-choroid interface during the active phase of CNV membrane formation, but absent in old quiescent scars.[24, 46] Our finding is consistent with those of previous studies showing that in patients with chronic inflammatory diseases such as keloids and sclerodermas, tenascin-C is expressed by fibroblasts.[47, 48] Therefore, it is likely that tenascin-C is continuously produced by myofibroblasts at the active edge of CNV in AMD patients and is not a transient phenomenon that peaks at 3 days.

The results of this study indicated that tenascin-C siRNA inhibited the formation of CNV *in vitro* and *in vivo*. Although aflibercept, a VEGF trap, is most commonly used for neovascular AMD (based on the clinical evidence),[6, 49] a recent report has suggested that the Fc portion of anti-VEGF drugs facilitates RPE cells transdifferentiation.[50] Our study demonstrated that transdifferentiation of hRPE cells into myofibroblasts results in the production of tenascin-C. These results suggest that aflibercept promotes CNV development via tenascin-C by facilitating RPE cell transdifferentiation. Therefore, aflibercept has a dual and conflicting mechanism of action; on one hand, it has anti-VEGF properties that inhibit CNV formation, and on the other hand, it may have pro-

angiogenic potential induced by tenascin-C from transdifferentiated RPE cells. These opposing effects may partially explain the tolerance or tachyphylaxis developed after long-term treatment with anti-VEGF drugs. Therefore, a combination of aflibercept and tenascin-C siRNA could exert a more potent effect on eyes with neovascular AMD, compared to singular aflibercept therapy.

In summary, we discovered that tenascin-C secreted from transdifferentiated RPE cells promotes CNV formation *in vitro* via integrin $\alpha_V\beta_3$, in a paracrine fashion. Furthermore, tenascin-C knock-out mice and mice that received a vitreous injection of tenascin-C siRNA showed a significant reduction in CNV volume. Therefore, tenascin-C could be an effective therapeutic target for combating AMD-associated CNV.

Acknowledgments

The authors would like to thank Masayo Eto for the technical assistance provided. This study was supported by Grants-in-Aid for Scientific Research (B) (No. 15H04995 and 26293374), a Grant-in-Aid for Challenging Exploratory Research (No. 26670757), and a Grant-in-Aid for JSPS Fellows from Japan Society for the Promotion of Science (No.15J03433).

Disclosure/Duality of interest

The authors have no disclosures/dualities of interest.

References

1 Lim LS, Mitchell P, Seddon JM, *et al.* Age-related macular degeneration. *The Lancet* 2012;379(9827):1728-1738.

2 Campochiaro PA, Soloway P, Ryan SJ, *et al.* The pathogenesis of choroidal neovascularization in patients with age-related macular degeneration. *Mol Vis* 1999;5:34.

3 Rosenfeld PJ, Brown DM, Heier JS, *et al.* Ranibizumab for neovascular age-related macular degeneration. *N Engl J Med* 2006;355(14):1419-1431.

4 Group CR, Martin DF, Maguire MG, *et al.* Ranibizumab and bevacizumab for neovascular age-related macular degeneration. *N Engl J Med* 2011;364(20):1897-1908.

5 Rofagha S, Bhisitkul RB, Boyer DS, *et al.* Seven-year outcomes in ranibizumab-treated patients in ANCHOR, MARINA, and HORIZON: a multicenter cohort study (SEVEN-UP). *Ophthalmology* 2013;120(11):2292-2299.

6 Schmidt-Erfurth U, Kaiser PK, Korobelnik JF, *et al.* Intravitreal aflibercept injection for neovascular age-related macular degeneration: ninety-six-week results of the VIEW studies. *Ophthalmology* 2014;121(1):193-201.

7 Schaal S, Kaplan HJ, Tezel TH. Is there tachyphylaxis to intravitreal anti-vascular endothelial growth factor pharmacotherapy in age-related macular degeneration? *Ophthalmology* 2008;115(12):2199-2205.

8 Binder S. Loss of reactivity in intravitreal anti-VEGF therapy: tachyphylaxis or tolerance? *Br J Ophthalmol* 2012;96(1):1-2.

9 Gasperini JL, Fawzi AA, Khondkaryan A, *et al.* Bevacizumab and ranibizumab tachyphylaxis in the treatment of choroidal neovascularisation. *Br J Ophthalmol* 2012;96(1):14-20.

10 Grunwald JE, Daniel E, Huang J, *et al.* Risk of geographic atrophy in the comparison of age-related macular degeneration treatments trials. *Ophthalmology* 2014;121(1):150-161.

11 Castellon R, Caballero S, Hamdi HK, *et al.* Effects of tenascin-C on normal and

diabetic retinal endothelial cells in culture. *Invest Ophthalmol Vis Sci* 2002;43(8):2758-2766.

12 Ishikawa K, Yoshida S, Kobayashi Y, *et al.* Microarray analysis of gene expression in fibrovascular membranes excised from patients with proliferative diabetic retinopathy. *Invest Ophthalmol Vis Sci* 2015;56(2):932-946.

13 Kobayashi Y, Yoshida S, Zhou Y, *et al.* Tenascin-C promotes angiogenesis in fibrovascular membranes in eyes with proliferative diabetic retinopathy. *Mol Vis* 2016;22:436-445.

14 Orend G, Chiquet-Ehrismann R. Tenascin-C induced signaling in cancer. *Cancer Lett* 2006;244(2):143-163.

15 Chiquet-Ehrismann R, Chiquet M. Tenascins: regulation and putative functions during pathological stress. *J Pathol* 2003;200(4):488-499.

16 Willems IE, Arends JW, Daemen MJ. Tenascin and fibronectin expression in healing human myocardial scars. *J Pathol* 1996;179(3):321-325.

17 Wallner K, Sharifi BG, Shah PK, *et al.* Adventitial remodeling after angioplasty is associated with expression of tenascin mRNA by adventitial myofibroblasts. *J Am Coll Cardiol* 2001;37(2):655-661.

18 Taki J, Inaki A, Wakabayashi H, *et al.* Dynamic expression of tenascin-C after myocardial ischemia and reperfusion: assessment by 125I-anti-tenascin-C antibody imaging. *J Nucl Med* 2010;51(7):1116-1122.

19 Garcion E, Faissner A, ffrench-Constant C. Knockout mice reveal a contribution of the extracellular matrix molecule tenascin-C to neural precursor proliferation and migration. *Development* 2001;128(13):2485-2496.

20 Tanaka K, Hiraiwa N, Hashimoto H, *et al.* Tenascin-C regulates angiogenesis in tumor through the regulation of vascular endothelial growth factor expression. *Int J Cancer* 2004;108(1):31-40.

21 Calvo A, Catena R, Noble MS, *et al.* Identification of VEGF-regulated genes associated with increased lung metastatic potential: functional involvement of tenascin-C in tumor growth and lung metastasis. *Oncogene* 2008;27(40):5373-5384.

22 Pezzolo A, Parodi F, Marimpietri D, *et al.* Oct-4+/Tenascin C+ neuroblastoma cells

serve as progenitors of tumor-derived endothelial cells. *Cell Res* 2011;21(10):1470-1486.

23 Grossniklaus HE, Green WR. Histopathologic and ultrastructural findings of surgically excised choroidal neovascularization. Submacular Surgery Trials Research Group. *Arch Ophthalmol* 1998;116(6):745-749.

24 Nicolo M, Piccolino FC, Zardi L*, et al.* Detection of tenascin-C in surgically excised choroidal neovascular membranes. *Graefes Arch Clin Exp Ophthalmol* 2000;238(2):107-111.

25 Nakama T, Yoshida S, Ishikawa K*, et al.* Inhibition of choroidal fibrovascular membrane formation by new class of RNA interference therapeutic agent targeting periostin. *Gene Ther* 2015;22(2):127-137.

26 Chang B, Hawes NL, Hurd RE*, et al.* Retinal degeneration mutants in the mouse. *Vision Res* 2002;42(4):517-525.

27 Lambert V, Lecomte J, Hansen S*, et al.* Laser-induced choroidal neovascularization model to study age-related macular degeneration in mice. *Nat Protoc* 2013;8(11):2197-2211.

28 Ishikawa K, Yoshida S, Nakao S*, et al.* Bone marrow-derived monocyte lineage cells recruited by MIP-1beta promote physiological revascularization in mouse model of oxygen-induced retinopathy. *Lab Invest* 2012;92(1):91-101.

29 Kobayashi Y, Yoshida S, Nakama T*, et al.* Overexpression of CD163 in vitreous and fibrovascular membranes of patients with proliferative diabetic retinopathy: possible involvement of periostin. *Br J Ophthalmol* 2015;99(4):451-456.

30 Yoshida S, Ishikawa K, Asato R*, et al.* Increased expression of periostin in vitreous and fibrovascular membranes obtained from patients with proliferative diabetic retinopathy. *Invest Ophthalmol Vis Sci* 2011;52(8):5670-5678.

31 Jin M, He S, Worpel V*, et al.* Promotion of adhesion and migration of RPE cells to provisional extracellular matrices by TNF-alpha. *Invest Ophthalmol Vis Sci* 2000;41(13):4324-4332.

32 Ishikawa K, Yoshida S, Nakao S*, et al.* Periostin promotes the generation of fibrous membranes in proliferative vitreoretinopathy. *FASEB J* 2014;28(1):131-142.

33 Amin R, Puklin JE, Frank RN. Growth factor localization in choroidal neovascular membranes of age-related macular degeneration. *Invest Ophthalmol Vis Sci* 1994;35(8):3178-3188.

34 Hanamura N, Yoshida T, Matsumoto E, *et al.* Expression of fibronectin and tenascin-C mRNA by myofibroblasts, vascular cells and epithelial cells in human colon adenomas and carcinomas. *Int J Cancer* 1997;73(1):10-15.

35 Imanaka-Yoshida K, Hiroe M, Nishikawa T, *et al.* Tenascin-C modulates adhesion of cardiomyocytes to extracellular matrix during tissue remodeling after myocardial infarction. *Lab Invest* 2001;81(7):1015-1024.

36 El-Karef A, Kaito M, Tanaka H, *et al.* Expression of large tenascin-C splice variants by hepatic stellate cells/myofibroblasts in chronic hepatitis C. *J Hepatol* 2007;46(4):664-673.

37 Pfeffer BA, Flanders KC, Guerin CJ, *et al.* Transforming growth factor beta 2 is the predominant isoform in the neural retina, retinal pigment epithelium-choroid and vitreous of the monkey eye. *Exp Eye Res* 1994;59(3):323-333.

38 Yuan F, Fu X, Shi H, *et al.* Induction of murine macrophage M2 polarization by cigarette smoke extract via the JAK2/STAT3 pathway. *PLoS One* 2014;9(9):e107063.

39 Cao X, Shen D, Patel MM, *et al.* Macrophage polarization in the maculae of age-related macular degeneration: a pilot study. *Pathol Int* 2011;61(9):528-535.

40 Gamulescu MA, Chen Y, He S, *et al.* Transforming growth factor beta2-induced myofibroblastic differentiation of human retinal pigment epithelial cells: regulation by extracellular matrix proteins and hepatocyte growth factor. *Exp Eye Res* 2006;83(1):212-222.

41 Ishikawa K, Kannan R, Hinton DR. Molecular mechanisms of subretinal fibrosis in age-related macular degeneration. *Exp Eye Res* 2015.

42 Kent D, Sheridan C. Choroidal neovascularization: a wound healing perspective. *Mol Vis* 2003;9:747-755.

43 Friedlander M, Theesfeld CL, Sugita M, *et al.* Involvement of integrins alpha v beta 3 and alpha v beta 5 in ocular neovascular diseases. *Proc Natl Acad Sci U S A* 1996;93(18):9764-9769.

44 Sriramarao P, Mendler M, Bourdon MA. Endothelial cell attachment and spreading on human tenascin is mediated by alpha 2 beta 1 and alpha v beta 3 integrins. *J Cell Sci* 1993;105 (Pt 4):1001-1012.

45 Johnson LV, Leitner WP, Staples MK, *et al.* Complement activation and inflammatory processes in Drusen formation and age related macular degeneration. *Exp Eye Res* 2001;73(6):887-896.

46 Fasler-Kan E, Wunderlich K, Hildebrand P, *et al.* Activated STAT 3 in choroidal neovascular membranes of patients with age-related macular degeneration. *Ophthalmologica* 2005;219(4):214-221.

47 Dalkowski A, Schuppan D, Orfanos CE, *et al.* Increased expression of tenascin C by keloids in vivo and in vitro. *Br J Dermatol* 1999;141(1):50-56.

48 Lacour JP, Vitetta A, Chiquet-Ehrismann R, *et al.* Increased expression of tenascin in the dermis in scleroderma. *Br J Dermatol* 1992;127(4):328-334.

49 Kumar N, Marsiglia M, Mrejen S, *et al.* Visual and anatomical outcomes of intravitreal aflibercept in eyes with persistent subfoveal fluid despite previous treatments with ranibizumab in patients with neovascular age-related macular degeneration. *Retina* 2013;33(8):1605-1612.

50 Chen CL, Liang CM, Chen YH, *et al.* Bevacizumab modulates epithelial-to-mesenchymal transition in the retinal pigment epithelial cells via connective tissue growth factor up-regulation. *Acta Ophthalmol* 2012;90(5):e389-398.

Figures legends

Figure 1. (a) Representative photographs of triple immunofluorescence staining for tenascin-C, α-smooth muscle actin (α-SMA), and CD34 in a choroidal neovascularization (CNV) membrane excised from an AMD patient. Tenascin-C staining was observed in α-SMA- and pan-cytokeratin-positive cells, and around CD34 positive cells.

(b) Triple immunofluorescence staining for tenascin-C, pan-cytokeratin, α-SMA, CD31, F4/80, and integrin α_V in lesions observed in a wild-type laser-induced CNV model 5 days post-laser treatment. Pan-cytokeratin-positive cells were stained with α-SMA. Tenascin-C co-stains with pan-cytokeratin, α-SMA, CD31, and integrin α_V, but not with F4/80. Nuclei are stained blue. Scale bar, 50 μm.

Figure 2. Kinetics of changes in mRNA (a) and protein (b) levels of tenascin-C in the retinal pigment epithelium (RPE)-choroid complex obtained from a mouse CNV model (mean ± SEM; n = 4 eyes per group).

(a, b) Tenascin-C expression is significantly increased and peaked 3 days after laser photocoagulation.

(c) Western blots of tenascin-C in the RPE-choroid complex of a mouse CNV model. The mouse monoclonal anti-tenascin-C clone 4F10TT antibody displayed 210 kDa- and 250 kDa-isoforms of tenascin-C, and a similar trend.

(d) Expression of tenascin-C mRNA normalized to GAPDH in human retinal pigment epithelial (hRPE) cells stimulated with the indicated concentrations of transforming growth factor-β2 (TGF-β2) (mean ± SEM; n = 4 per group).

(e) ELISA of tenascin-C in the cell lysates and supernatants of hRPE cells stimulated with the indicated concentrations TGF-β2 (mean ± SEM; n = 4 per group).

(d, e) TGF-β2 significantly induces the expression of tenascin-C mRNA and protein, in a dose-dependent manner.

(f) Western blot analysis of tenascin-C and β-actin in hRPE cells stimulated by the indicated concentrations of TGF-β2. The mouse monoclonal anti-tenascin-C clone 4F10TT antibody showed two isoforms of tenascin-C (210 and 300 kDa) and a similar trend. β-actin was used as the loading control. *$P < 0.05$, **$P < 0.01$, ANOVA/Dunnett's test, compared to the control.

Figure 3. Effect of tenascin-C on proliferation (a) and adhesion (b, c) of hRPE cells and proliferation (d), adhesion (e, f), migration (g), and tube formation (h, i) of human microvascular endothelial cells (HMVECs).

(a) hRPE cell proliferation was assessed by bromodeoxyuridine (BrdU) incorporation (mean ± SEM; n = 4 per group). hRPE cell proliferation was significantly increased by tenascin-C in a dose-dependent manner.

(b, c) hRPE cells were incubated with the indicated concentrations of tenascin-C or TGF-β2 (positive control) in fibronectin-coated 96-well plates for 1 hour (mean ± SEM; n = 4 per group) to analyze the cell adhesion. hRPE cell adhesion was significantly up-

regulated by TGF-β2 (10 ng/mL) and down-regulated by tenascin-C (300 ng/mL). Photographs were taken with a 20× objective after Hoechst 33342 staining.

(d) HMVECs were incubated with the indicated concentrations of tenascin-C for 24 hours to assess proliferation (mean ± SEM; n = 4 per group).

(e, f) HMVECs were incubated with the indicated concentrations of tenascin-C in fibronectin-coated 96-well plates for 12 hours to assess adhesion (mean ± SEM; n = 4 per group).

(g) HMVECs stimulated with tenascin-C were placed in the upper chamber and allowed to migrate to the reverse side of the membrane to assess the cell migration (mean ± SEM; n = 4 per group).

(h, i) HMVECs were seeded on a basement membrane (BM) matrix with the indicated concentrations of tenascin-C (mean ± SEM; n = 6 per group). Tubes formed by HMVECs were photographed after incubating for 12 hours (4× objective).

(d–i) Tenascin-C significantly increased the HMVEC proliferation, adhesion, migration, and tube formation, in a dose-dependent manner. Values are expressed as a percentage relative to the untreated control. **P* < 0.05, ***P* < 0.01, ANOVA/Dunnett's test.

Figure 4. Inhibitory effect of cilengitide on tenascin-C-induced proliferation, adhesion, migration, and tube formation in HMVECs.

(a) HMVECs were incubated with tenascin-C (300 ng/mL) and cilengitide (10 μM) for 24 h.

(b, c) Cell adhesion was assessed by incubating the HMVECs with tenascin-C (300 ng/mL) and cilengitide (10 μM) on fibronectin-coated 96-well plates for 12 hours (mean ± SEM; n = 4 per group).

(d) The cell migration was assessed placing HMVECs stimulated with tenascin-C (300 ng/mL) and cilengitide (10 μM) in the upper chamber and allowing the cells to migrate to the other side of the membrane (n = 4 per group).

(e, f) HMVECs were seeded on BM matrix with tenascin-C (300 ng/mL) and cilengitide (10 μM) (mean ± SEM; n = 6 per group). Tubes formed by HMVECs were photographed after a 12-hour incubation period (4× objective).

(a–f) Cilengitide significantly inhibited tenascin-C-induced proliferation, adhesion, migration, and tube formation of HMVECs. Values are expressed as a percentage relative to the control. *$P < 0.05$, **$P < 0.01$, ANOVA/Dunnett's test.

Figure 5. Inhibitory effect of tenascin-C siRNA on HMVEC proliferation and tube formation, induced by conditioned medium of hRPE cells treated with TGF-β2.

(a) Tenascin-C expression in the conditioned medium of hRPE cells transfected with tenascin-C siRNA. Following transfection with tenascin-C or control siRNA (10 nM), hRPE cells were treated with or without TGF-β2 (10 ng/mL) for 24 hours (mean ± SEM; n = 4 per group). Tenascin-C siRNA significantly reduced the concentration of tenascin-C in the conditioned medium of hRPE cells treated with TGF-β2.

(b) HMVECs were incubated to assess proliferation in hRPE-conditioned medium for 24 hours.

(c, d) HMVECs were seeded on BM matrix in hRPE-conditioned medium (mean ± SEM; n = 6 per group). Tube formed by HMVECs were photographed after a 12-hour incubation period (4× objective).

(b–d) HMVECs cultured in hRPE-conditioned medium transfected with tenascin-C siRNA after TGF-β2 stimulation showed a significant reduction in proliferation and tube formation compared to the control cells. Values are expressed as a percentage relative to the control. *$P < 0.05$, **$P < 0.01$, ANOVA/Tukey test.

Figure 6. Volume of CNV formed after laser photocoagulation in tenascin-C knock-out mice and mice treated with tenascin-C siRNA.

(a) Analysis of the volume of CNV lesions 7 days after photocoagulation in wild-type and tenascin-C knock-out mice (mean ± SEM; n = 8 eyes per group).

(b) Representative projections (green) and 3D images (red) of CNV lesions. Scale bar, 100 μm.

(a, b) CNV volume was significantly smaller in the eyes of tenascin-C knock-out mice compared to that in wild-type mice.

(c) Analysis of the volume of CNV lesions 7 days after vitreous injection of control siRNA or tenascin-C siRNA (mean ± SEM; n = 8 eyes per group).

(d) Representative projections (green) and 3D images (red) of CNV lesions. Scale bar, 100 μm.

(c, d) CNV volume was significantly lower in eyes treated with tenascin-C siRNA (10 and 100 nM) compared to that in eyes treated with control siRNA. *$P < 0.05$, **$P < 0.01$, Student's *t* test or ANOVA/Dunnett's test.

Figure 1

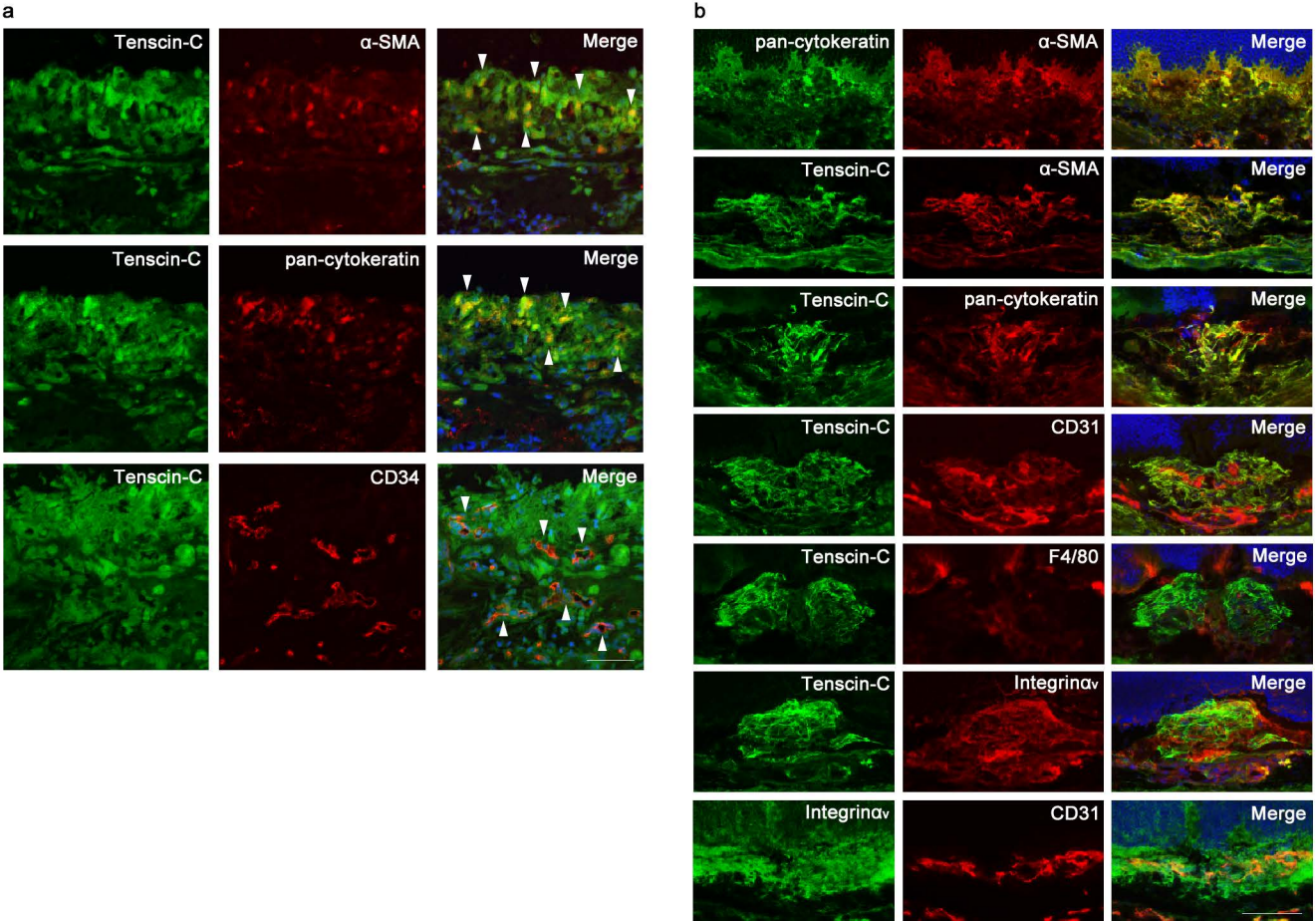
a
Tenscin-C
α-SMA
Merge
Tenscin-C
pan-cytokeratin
Merge
Tenscin-C
CD34
Merge
b
pan-cytokeratin
α-SMA
Merge
Tenscin-C
α-SMA
Merge
Tenscin-C
pan-cytokeratin
Merge
Tenscin-C
CD31
Merge
Tenscin-C
F4/80
Merge
Tenscin-C
Integrinαv
Merge
Integrinαv
CD31
Merge

Figure 2

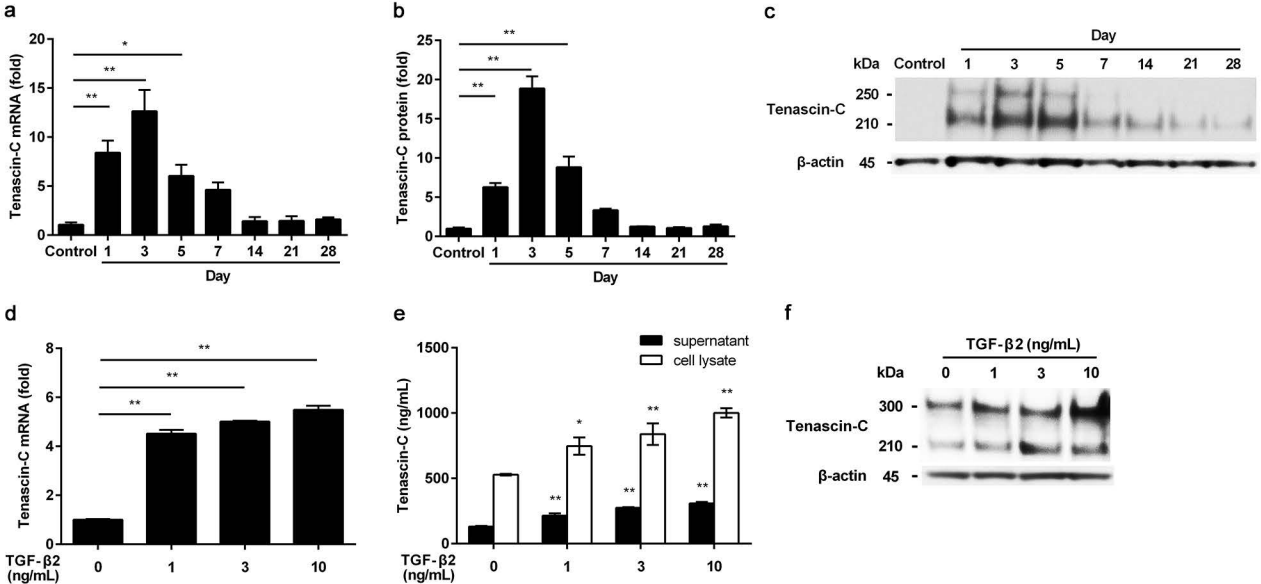
a
Tenascin-C mRNA (fold)
Control 1 3 5 7 14 21 28
Day
b
Tenascin-C protein (fold)
Control 1 3 5 7 14 21 28
Day
c
Day
kDa Control 1 3 5 7 14 21 28
Tenascin-C
250
210
β-actin 45
d
Tenascin-C mRNA (fold)
TGF-β2 (ng/mL) 0 1 3 10
e
supernatant
cell lysate
Tenascin-C (ng/mL)
TGF-β2 (ng/mL) 0 1 3 10
f
TGF-β2 (ng/mL)
kDa 0 1 3 10
Tenascin-C
300
210
β-actin 45

Figure 3

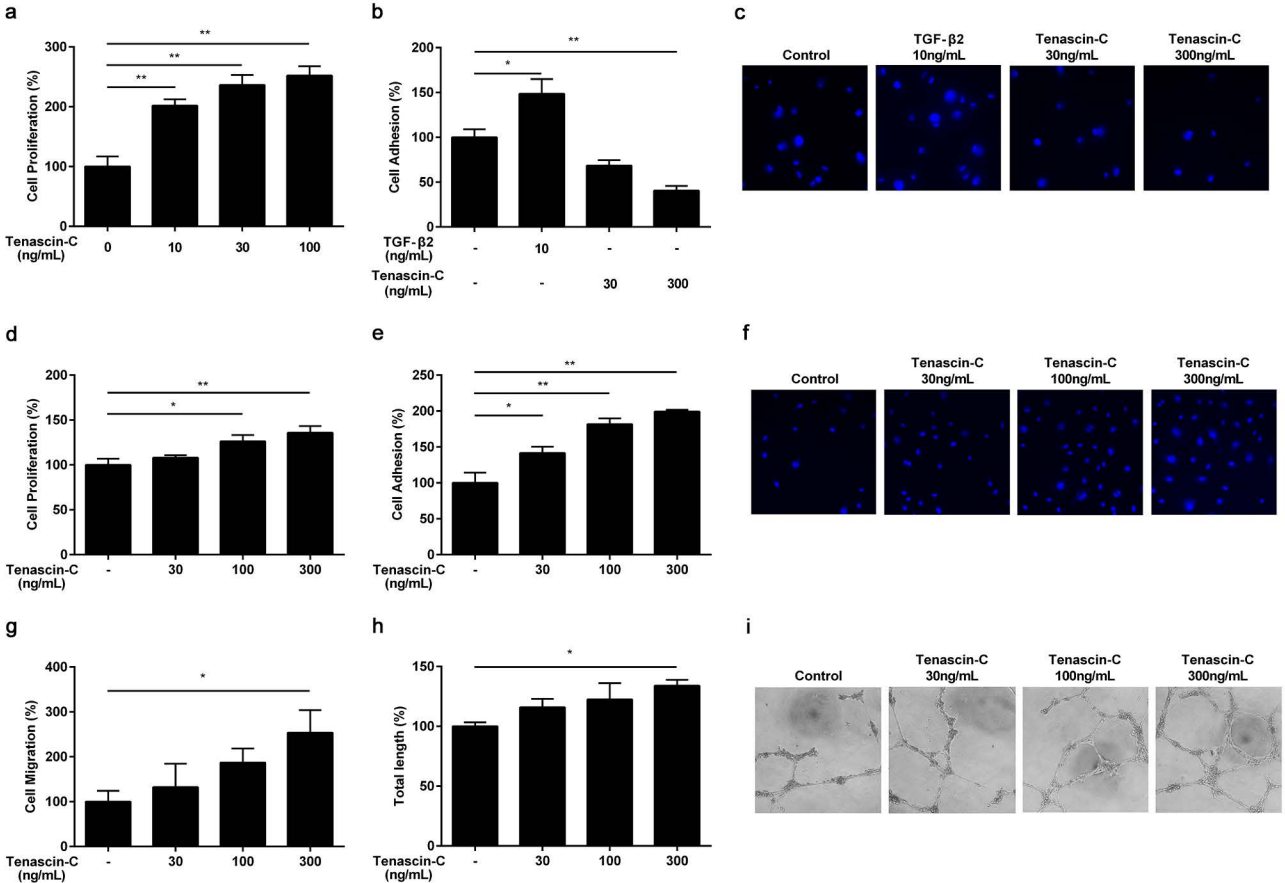
a
Cell Proliferation (%)
300
200
100
0
**
**
**
Tenascin-C (ng/mL)
0
10
30
100
b
Cell Adhesion (%)
200
150
100
50
0
**
*
TGF-β2 (ng/mL)
-
10
-
-
Tenascin-C (ng/mL)
-
-
30
300
c
Control
TGF-β2 10ng/mL
Tenascin-C 30ng/mL
Tenascin-C 300ng/mL
d
Cell Proliferation (%)
200
150
100
50
0
**
*
Tenascin-C (ng/mL)
-
30
100
300
e
Cell Adhesion (%)
250
200
150
100
50
0
**
**
*
Tenascin-C (ng/mL)
-
30
100
300
f
Control
Tenascin-C 30ng/mL
Tenascin-C 100ng/mL
Tenascin-C 300ng/mL
g
Cell Migration (%)
400
300
200
100
0
*
Tenascin-C (ng/mL)
-
30
100
300
h
Total length (%)
150
100
50
0
*
Tenascin-C (ng/mL)
-
30
100
300
i
Control
Tenascin-C 30ng/mL
Tenascin-C 100ng/mL
Tenascin-C 300ng/mL

Figure 4

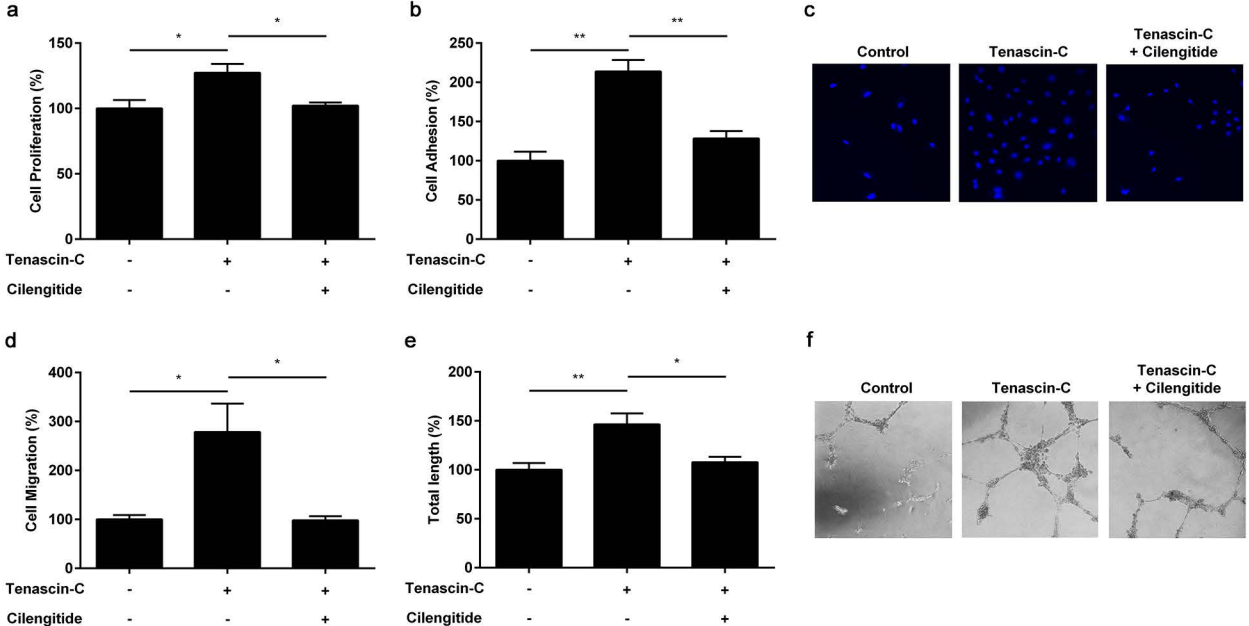
a
Cell Proliferation (%)
150
100
50
0
*
*
Tenascin-C - + +
Cilengitide - - +
b
Cell Adhesion (%)
250
200
150
100
50
0
**
**
Tenascin-C - + +
Cilengitide - - +
c
Control
Tenascin-C
Tenascin-C + Cilengitide
d
Cell Migration (%)
400
300
200
100
0
*
*
Tenascin-C - + +
Cilengitide - - +
e
Total length (%)
200
150
100
50
0
**
*
Tenascin-C - + +
Cilengitide - - +
f
Control
Tenascin-C
Tenascin-C + Cilengitide

Figure 5

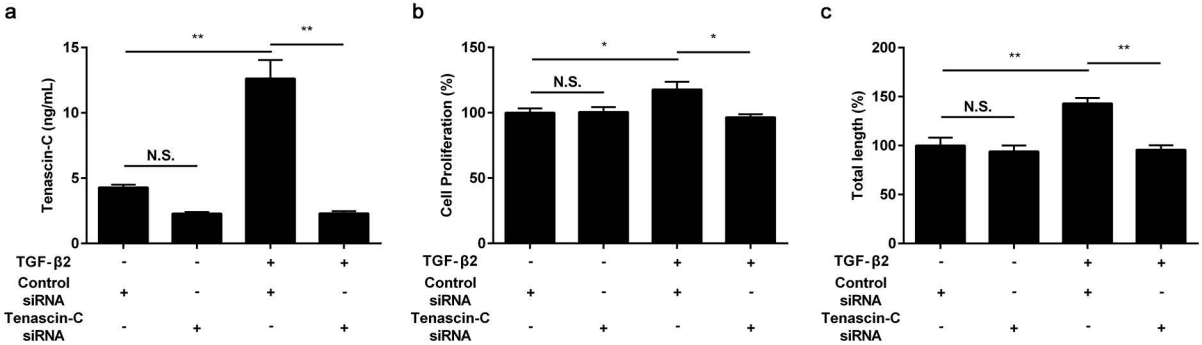
a
Tenascin-C (ng/mL)
15
10
5
0
**
**
N.S.
TGF-β2 - - + +
Control siRNA + - + -
Tenascin-C siRNA - + - +
b
Cell Proliferation (%)
150
100
50
0
*
*
N.S.
TGF-β2 - - + +
Control siRNA + - + -
Tenascin-C siRNA - + - +
c
Total length (%)
200
150
100
50
0
**
**
N.S.
TGF-β2 - - + +
Control siRNA + - + -
Tenascin-C siRNA - + - +

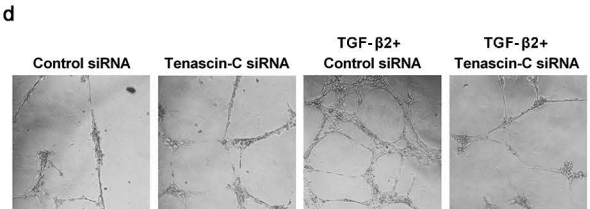
d
Control siRNA
Tenascin-C siRNA
TGF-β2+ Control siRNA
TGF-β2+ Tenascin-C siRNA

Figure 6

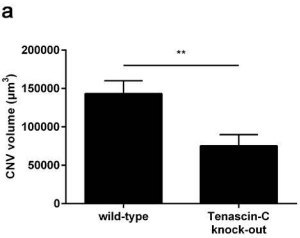
a
200000
150000
100000
50000
0
CNV volume (μm3)
**
wild-type
Tenascin-C knock-out

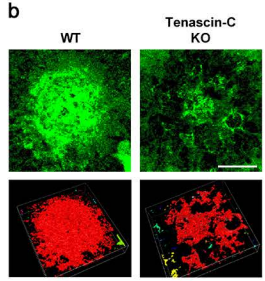
b
WT
Tenascin-C KO

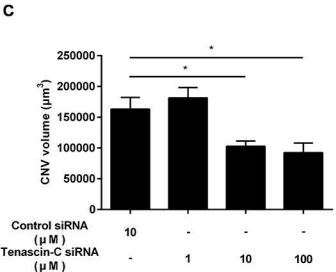
c
250000
200000
150000
100000
50000
0
CNV volume (μm3)
*
*
Control siRNA (μM)
Tenascin-C siRNA (μM)
10
-
-
-
-
1
10
100

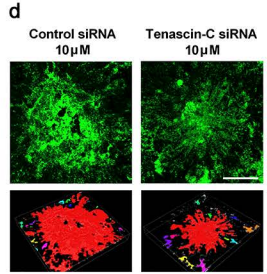
d
Control siRNA 10μM
Tenascin-C siRNA 10μM

Supplementary Table 1. List of antibodies used in immunofluorescence staining for CNV membranes

Antibody name	Company	dilution
Anti-tenascin-C	supplied by Juntendo University	20μg/mL
Anti-α-smooth muscle actin	Sigma-Aldrich (C6198)	1:250
Anti-pan-cytokeratin	Dako (M3515 and M7010)	1:50
Anti-CD34	Leica Biosystems (NCL-L-END)	1:2000
Anti-rat Alexa Fluor 488	Life Technologies (A11006)	1:800
Anti-mouse Alexa Fluor 647	Life Technologies (A21247)	1:800

Supplementary Table 2. List of antibodies used in immunofluorescence staining for CNV model

Antibody name	Company	dilution
Anti-tenascin-C	IBL (10337)	1:200
Anti-α-smooth muscle actin	Abcam (ab21027)	1:50
Anti-pan-cytokeratin	Santa Cruz Biotechnology (sc8018)	1:100
Anti-CD31	BD Biosciences (550274)	1:100
Anti-F4/80	BioLegend (123121)	1:100
Anti-integrin α_V	Millipore (AB1930)	1:1000
Anti-mouse Alexa Fluor 488	Life Technologies (A11001)	1:200
Anti-rabbit Alexa Fluor 488	Life Technologies (A21206)	1:200
Anti-rat Alexa Fluor 647	Life Technologies (A21247)	1:200
Anti-goat Alexa Fluor 647	Life Technologies (A21469)	1:200
Anti-rabbit Alexa Fluor 647	Life Technologies (A21244)	1:200

Supplementary Table 3. List of PCR primers and annealing temperatures

Genes	Primer and Probe	T_{anneal}
Tenascin-C	Hs01115665_m1 (Thermo Fisher Scientific)	60
GAPDH	forward: 5'-GAGTCAACGGATTTGGTCGT-3'	60
	reverse: 5'-CTTGATTTTGGAGGGATCTCGC-3'	

Supplementary Table 4. List of siRNA sequences

Genes	Sequence
Tenascin-C	sense: 5'-CUGAAAUUGGAAACUUAAATT-3'
	antisense: 5'-UUUAAGUUUCCAAUUUCAGTT-3'